Reliability-Based Design of the Foundation of an Offshore Wind Energy Converter using the Single Surface Hardening Model

A. Kisse & K. Lesny
Instiute of Soil Mechanics and Foundation Engineering, University of Duisburg-Essen, Germany

ABSTRACT: Based on a new model which describes the behaviour of shallow foundations over the whole loading range up to the ultimate state and the Hasofer-Lind second moment reliability index ß a reliability design method is presented. The model includes a failure condition defining the ultimate bearing capacity and a corresponding displacement rule describing the system behaviour under serviceability conditions. Using the example of an offshore wind energy converter the influence of individual load combinations on the safety of the system taking into account scatter and correlations of the parameters is examined.

1 INTRODUCTION

In knowledge of the limitation of fossile fuels the German policy supports the development and utilisation of renewable energies. In this connection the expansion of wind energy is planned. Because the possibilities for the expansion of onshore wind energy are limited, the developments have to go offshore. Currently several design concepts for the foundation of such offshore wind energy converters in the north sea and baltic sea are investigated (Wiemann et al. 2002). Here the design of a gravity foundation will be discussed (Fig. 1).

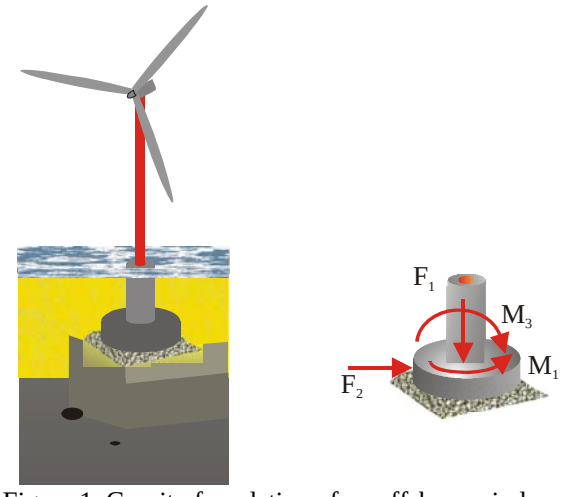

Figure 1. Gravity foundation of an offshore wind energy converter

The calculation is conducted by assuming the extreme loads as quasi-static loads for the analysis of the ulimate state (ULS) and the serviceability state (SLS) within foundation design. This way follows the design concept by Lesny & Hinz (2006) in which the dimension of the foundation will be verifed with quasi-static loads and in a following step under cyclic loading.

In today's codes of practice, e. g. Eurocode 7 (2004) different ultimate limit states and serviceability limit states have to be distinguished. Only with difficulties the crucial load combination can be determined and thus the safety of the system, especially because a three-dimensional load problem is concerned here (Fig. 1). In contrast to this, the Single Surface Hardening Model (SSH-Model) combines the serviceability limit state and the ultimate limit state. It describes the relationship between loading up to failure and corresponding displacements of the foundation by a consistent formulation, so that the distinction between different limit states is no longer necessary.

This concept allows for a clear definiton of safety and provides a distinct basis for the application of probabilistic methods. In this paper such a probabilistic design on basis of the very practicable Hasofer-Lind index is presented. The influences of individual load combinations on the safety of the system taking into account scatter and correlations of the parameters are examined.

2 SINGLE SURFACE HARDENING MODEL

The concept of the SSH-Model includes two components. The first component is a failure condition which describes the ULS of a shallow foundation without distinguishing different failure

modes. The second component is a displacement rule which reflects the complete load-displacement relation before the system reaches its ultimate limit state, thus integrating the SLS.

2.1 *Failure condition*

In analogy to the concept of constitutive laws of plasticity the failure condition consistently describes the ultimate bearing capacity of the foundation similar to a yield condition. Hence, all the former isolated ultimate limit states (for shallow foundations: base failure, sliding, uplift and limitation of eccentricity) are integrated into an unique limit state equation. So for the design of foundations it needs to be checked only if the loadpath is located inside the failure surface or not (Fig. 2).

Generally, a single footing is loaded by a vertical load F_1, horizontal load components F_2 and F_3, a torsional moment M_1 and bending moment components M_2 and M_3 (Fig. 3). The load components are summarized in the load vector:

$$\vec{Q}^T = \left[F_1\, F_2\, F_3\, M_1\, M_2\, M_3\right] \tag{1}$$

In the basic case (c = 0, d = 0) the geometry of the footing described by the side ratio b_2/b_3, weight γ, shear strength φ'of the soil and a quantity μ_S describing the roughness of the footing base have to be considered (Fig. 3).
With these input parameters the failure condition of the general form

$$F\left(\vec{Q}, b_2/b_3, \gamma, \tan\varphi', \mu_S\right) = 0 \tag{2}$$

has been defined by Equation 3.

The quantity F_{10} represents the resistance of a footing under pure vertical loading which can be calculated using traditional bearing resistance formula (DIN EN 1997-1 2005).

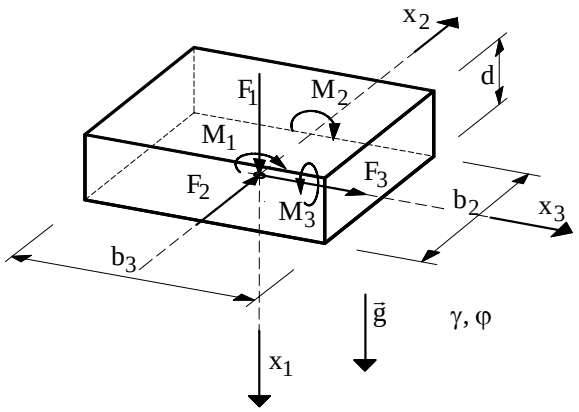

Figure 3. Geometry and loading

$$F = \sqrt{\frac{F_2^2 + F_3^2}{\left(a_1 \cdot F_{10}\right)^2} + \frac{M_1^2}{\left(a_2 \cdot \left(b_2 + b_3\right) \cdot F_{10}\right)^2} + \frac{M_2^2}{\left(a_3 \cdot b_3 \cdot F_{10}\right)^2} + \frac{M_3^2}{\left(a_3 \cdot b_2 \cdot F_{10}\right)^2}} - \frac{F_1}{F_{10}} \cdot \left(1 - \frac{F_1}{F_{10}}\right)^{\alpha} = 0 \tag{3}$$

The parameters a_i govern the inclination of this failure surface for small vertical loading where the limit states sliding and overturning have been relevant (see Fig. 2). These limit states are integrated by the following formulations of the parameters a_i and α:

$$a_1 = \pi/2 \cdot \mu_S \cdot \tan\varphi' \cdot e^{-\pi/3 \cdot \tan\varphi'}$$

$$a_2 = 0.098,\ a_3 = 0.42,\ \alpha = 1.3 \tag{4}$$

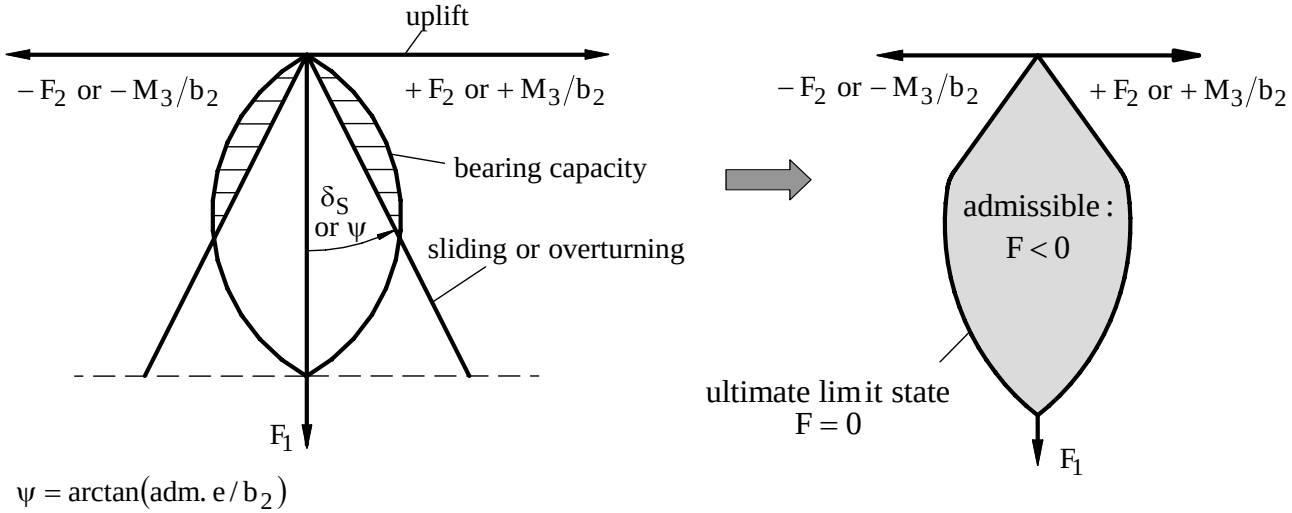

Figure 2. Resultant ultimate bearing capacity of a foundation in the loading space (Lesny & Richwien 2002)

The parameter α controls the position of the maximum of the failure surface.

The limit state uplift is already included in Equation 3, because only positive vertical loads are admissible. The parameters have been derived from an analysis of numerous small scale model tests conducted at our institute (Lesny 2001, Lesny & Richwien 2002).

2.2 *Displacement Rule*

The failure condition spreads out a failure surface which represents the outer border of the loading (Fig. 4). So the displacements u_i and rotations ω_i of the foundation are caused by arbitrary loading inside the failure surface. They are described by the displacement rule and summarized in a displacement vector:

$$\vec{u}^{\,T} = \left[u_1\ u_2\ u_3\ \omega_1\ \omega_2\ \omega_3\right]^T \tag{5}$$

Due to the complex interaction of load components, displacements and rotations the displacement rule has been formulated using the well-known strain hardening plasticity theory with isotropic hardening (e. g. Zienkiewicz 1988). Hence, displacements and rotations are calculated according to Equation 6, assuming that all deformations are plastic.

$$d\vec{u} = \frac{1}{H}\cdot\left(\frac{\partial F}{\partial \vec{Q}}\right)^T \cdot \frac{\partial G}{\partial \vec{Q}}\cdot \Delta\vec{Q} \tag{6}$$

The components of the displacement rule are a yield surface described by the yield condition F:

$$F\left(\vec{Q}, F_a\right) = \sqrt{\frac{F_2^2+F_3^2}{\left(a_1\cdot F_a\right)^2} + \frac{M_1^2}{\left(a_2\cdot\left(b_2+b_3\right)\cdot F_a\right)^2} + \frac{M_2^2}{\left(a_3\cdot b_3\cdot F_a\right)^2} + \frac{M_3^2}{\left(a_3\cdot b_2\cdot F_a\right)^2}} - \frac{F_1}{F_a}\cdot\left(1-\frac{F_1}{F_a}\right)^{\alpha} = 0 \tag{7}$$

with the parameters a_i and α of Equation 4, a plastic potential G:

$$G\left(\vec{Q}, F_b\right) = \sqrt{\frac{F_2^2+F_3^2}{\left(c_1\cdot F_b\right)^2} + \frac{M_1^2}{\left(c_2\cdot\left(b_2+b_3\right)\cdot F_b\right)^2} + \frac{M_2^2}{\left(c_3\cdot b_3\cdot F_b\right)^2} + \frac{M_3^2}{\left(c_3\cdot b_2\cdot F_b\right)^2}} - \frac{F_1}{F_b}\cdot\left(1-\frac{F_1}{F_b}\right)^{\alpha} = 0 \tag{8}$$

and a strain-hardening function H:

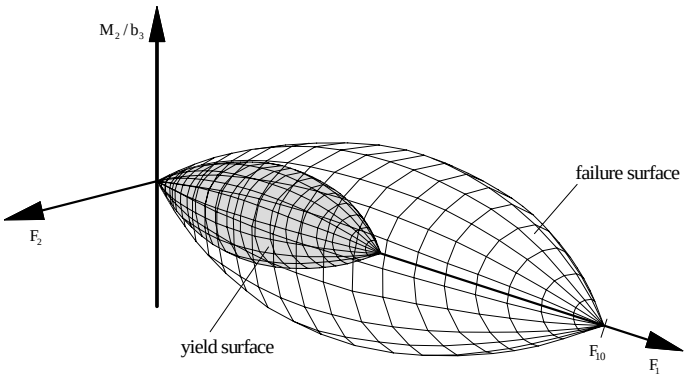

Figure 4. Isotropic expansion of the yield surface in the 3 dimensional loading space

$$H = -\frac{\partial F\left(\vec{Q}, F_a\right)}{\partial F_a}\cdot\frac{\partial F_a}{\partial \vec{u}}\cdot\frac{\partial G\left(\vec{Q}, F_b\right)}{\partial \vec{Q}} \tag{9}$$

The yield surface expands due to isotropic hardening until the failure surface defined by the failure condition is reached (Fig. 4). Thus, the parameters c_i and ß in Equation 8 have to be determined as functions of a_i and α, respectively.

The expansion of the yield surface depends mainly on the vertical displacement which itself depends on the degree of mobilization of the maximum resistance F_{10}. Hence, it is sufficient enough to define the hardening parameter F_a as a function of these two quantities according to (Bay-Gress 2000):

$$F_a = \left(F_{10} + k_f\cdot u_1\right)\cdot\left\{1-\exp\left(\frac{-k_0\cdot u_1}{F_{10}+k_f\cdot u_1}\right)\right\} \tag{10}$$

The initial and final stiffness of the corresponding load-displacement curve, k_0 and k_f respectively, may be determined using a method proposed by Mayne & Poulos (2001) in which the soil stiffness can be determined by any standard procedure.

The complex load-displacement behaviour of the foundations under various loading situations can be represented best by a tensorial function (Lesny et al. 2002):

$$d\vec{u} = \underline{K}\cdot d\vec{Q} \tag{11}$$

Here, the compliance matrix can be derived from the formulation in Equation 6:

$$\underline{K} = \frac{1}{H}\cdot\left(\frac{\partial F}{\partial \vec{Q}}\right)^T \cdot \frac{\partial G}{\partial \vec{Q}} \tag{12}$$

So the matrix $\underline{K}$ defines the relation between the loading and the corresponding deformations and rotations.

As an example the simulation of two small scale model tests with an inclined loading using the SSH-Model is shown in Figures 5 and 6. The tests were

carried out by Montrasio (1994) on dense Ticino sand (D = 0.94) with a load inclination of δ = 3° and 8°. The footing dimensions is $b_2 = b_3 = 80$ mm. Here the theoretical load settlement curves lies below the experimental curves. Due to the fact that the theoretical failure load F_{10} is smaller than the load from the test the stiffness k_0 after Equation 10 is also smaller. So the slope of the curve is steeper and the settlements are overestimated.

Altogether a good agreement of the theoretical curve with the experimental curves is shown.

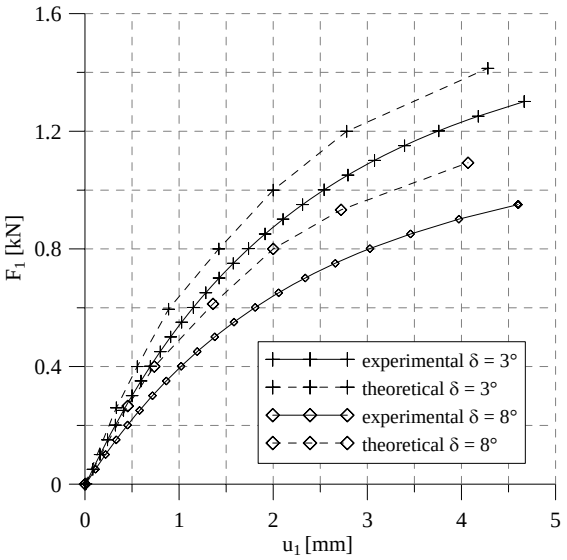

Figure 5. Simulation of a small scale model test with inclined loading on dense Ticino sand, $u_1 - F_1$ curves

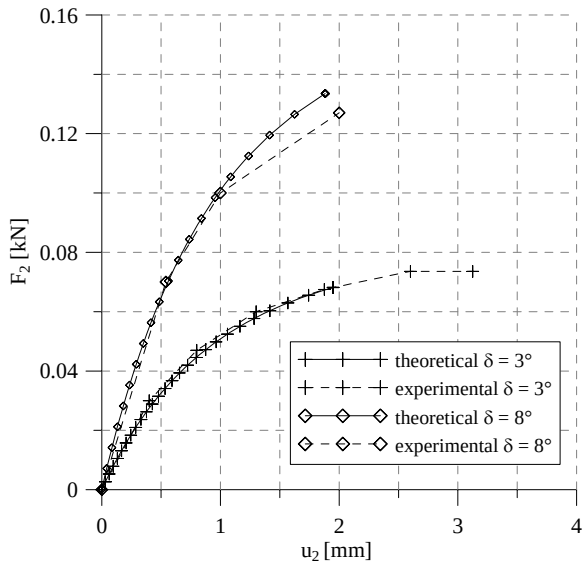

Figure 6. Simulation of two small scale model tests with inclined loading on dense Ticino sand, u_2 - F_2 curves

3 HASOFER-LIND INDEX ß

As shown before the failure condition of the model spreads out a failure surface which represents the outer border of the permissible loading. Hence the distance of the actual loading from the failure surface describes the safety of the system.

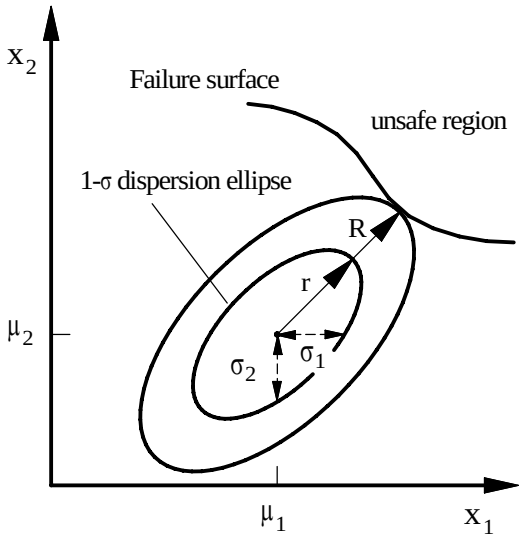

Figure 7. Illustration of reliability index ß in the plane (after Low 2005)

This safety can be determined easily using reliability analysis. Here, the Hasofer-Lind second moment reliability index ß will be evaluated. In this context, safety is the shortest distance from the safe mean-value point to the most probable combination of parameters on the failure surface (Fig. 7).

For practical applications the methods proposed by Low & Tang (1997 & 2004) and Phoon (2004) are especially suitable for the determination of the index ß. Within these methods object-oriented constrained optimization in the spreadsheet platform is used. With this formulation it is possible to indicate the safety of the system not only for the mean values but also in dependence of scatter and correlations of the parameters.

The matrix form of the Hasofer-Lind reliability index is (after Low & Phoon 2002):

$$ß = \min_{\underline{x} \in F} \sqrt{\left(\frac{x_i - \mu_i}{\sigma_i}\right)^T \cdot \underline{R}^{-1} \cdot \left(\frac{x_i - \mu_i}{\sigma_i}\right)} \qquad (13)$$

where $\underline{x}$ is a vector representing the set of random variables x_i, μ_i are the mean values, $\underline{R}$ is the correlation matrix, σ_i is the standard deviation and F the failure domain.

The interpretation from Low & Tang (1997) of the H-L index describes a tilted multidimensional ellipsoid (centered at the mean) in the original space of the random variables (Fig. 7). This ellipsoid will be expanded until it touches the limit state surface. This point describes the most probable failure combination of the parameters. So the index ß can be explained as the ratio of the radius r of the 1-σ ellipsoid to the radius R of the expanded ellipsoid

$$ß = \min\left(\frac{R}{r}\right) \qquad (14)$$

and safety is measured by the shortest distance from the safe mean-value point to the most probable failure combination of parameters on the limit state surface.

The following calculations are performed using Microsoft Excel software and its built-in optimisation program Solver. The computations followed the spreadsheet formulations of Low & Tang (1997) and Low & Phoon (2002).

4 RELIABILITY-BASED GRAVITY FOUNDATION DESIGN

With the load combination in Figure 1 and the limit state surface formulated after Equation 3 a reliabilty design for a gravity foundation will be performed. Figure 9 shows the general spreadsheet for the analysis.

4.1 *Simple example with two correlated normals*

For a better understanding a simpler case will be considered first. Therefore, only the loads F_2 and M_1, which are normally distributed, are taken into account. All other parameters are fixed. In this case the failure surface is constant in the loading space (F_{10} = const.). Now it is possible to cut the failure surface along the F_1-axis and take a view of the effect of the correlations of the loads F_2 and M_1 (Fig. 8). If the two variables are uncorrelated the ellipse is cononical (i.e. non-tilted). In opposite if the loads are correlated the ellipses are tilted. For positive correlation factors they are positivity tilted and for negative values they are negativity tilted.

Generally the index ß and so the safety of the system presented here depends on the correlation factor. For the case the index ß is the same for all correlations. That means, that the distance between the ellipse for different values of ρ and the failure surface (for F_1 = 60 MN) is the same. This is due to the fact that the failure surface is a straight line and not a curved line here. So the index ß for all ellipses is ß = 2.786.

On the other hand the example allows to consider the influence of the vertical load F_1. Therefore the failure surface from Figure 4 is cut at two additional different values of F_1 (F_1 = 40 and 80 MN). Figure 8 shows the failure lines in the F_1 - M_1-plane.

For F_1 = 40 MN the failure line cut the 1-σ ellipse and so the safety of the system become smaller 1. In the other case the index ß becomes greater, visible by the increasing distance between the 1-σ ellipse and the failure line in Figure 8. So with increasing the vertical load it is possible to increase the saftey of the system. If the vertical load is getting higher and higher the safety descrease again and the failure mode moves from a sliding mode over to a bearing

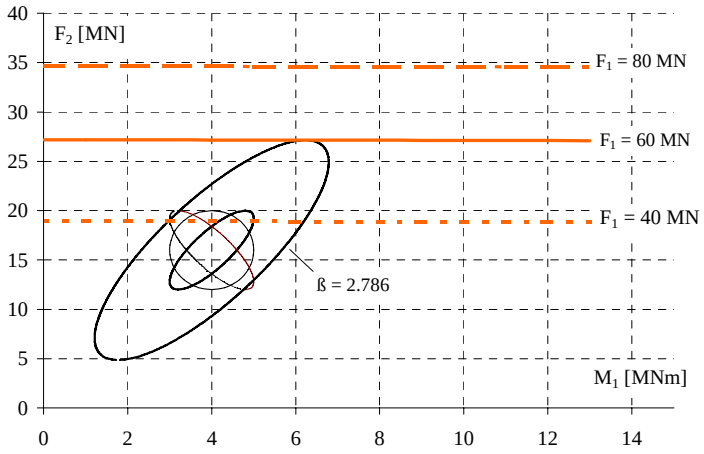

Figure 8. Rotation of the 1-σ disperison ellipsiod and failure lines for different vertical loads F_1

failure mode. Released through the moving of the F_2 - M_1 - plane over the bulge of the failure surface the distance between the 1-σ ellipse to the failure surface reduces again.

4.2 *N dimensional example*

In the general case three loads have to be taken into account (Fig. 9) because the vertical load, which contains the weight of the turbine and the gravity foundation, is assumed to be constant. The diameter of the foundation is D = 20 m and the height H = 10 m. The coefficient of variation for the loads is equal to 0.25 and for the vertical failure load F_{10} 0.15. The COV for resistance parameters a_i is 0.1 and for the soil parameters 0.08. All variables are assumed to be normally distributed.

Some correlations parameters are assumed, as shown in the correlation matrix. The correlation between φ and F_{10} is logic, because the failure load after pREN 1997-1 (2004) depends on the soil friction angle. Also a_1 depends on this value and the roughness of the footing base μ. Since a_2 and a_3 were selected as adjustment values, which do not exhibit dependence to geometry or the soil parameters, are not correlated.

The PerFunc is the failure condition after Equation 3 and the column labeled nx contains the Equation:

$$nx_i = \frac{x_{ki} - \mu_i}{\sigma_i} \qquad (15)$$

The x_k column denotes the point where the 9-dimensional equivalent dispersion ellipsoid touches the limit state surface. By comparing either the ratios under the nx column, it is evident that the bearing capacity depence more on M_3 than on F_2 or M_1. This occurs also in the parameters a_i. Here the response is far more sensitive to a_3 than to a_1 or a_2. Likewise the influence of the failure load F_{10} is very small. This is

H	D	b_2	b_3	F_1	α
[m]	[m]	[m]	[m]	[MN]	[-]
10	20	17,72	17,72	125	1,3

normally distributed variables

	X_k		μ mean	σ StDev	nx
M_3	661,66	[MNm]	562	85	1,17252
M_1	4,20	[MNm]	4	1	0,201
F_2	17,00	[MN]	16	4	0,25108
φ' (tan)	0,69	[-]	0,7	0,05	-0,2232
μ	0,79	[-]	0,8	0,06	-0,0841
F_{10}	918,43	[MN]	969,6	150	-0,3411
a_1	0,51	[-]	0,514	0,05	-0,105
a_2	0,10	[-]	0,098	0,01	-0,0001
a_3	0,38	[-]	0,42	0,04	-0,9564

Correlation matrix

	M_3	M_1	F_2	φ' (tan)	μ	F_{10}	a_1	a_2	a_3
M_3	1	0	0	0	0	0	0	0	0
M_1	0	1	0,8	0	0	0	0	0	0
F_2	0	0,8	1	0	0	0	0	0	0
φ' (tan)	0	0	0	1	0,8	0,5	0,5	0	0
μ	0	0	0	0,8	1	0	0,8	0	0
F10	0	0	0	0,5	0	1	0	0	0
a_1	0	0	0	0,5	0,8	0	1	0	0
a_2	0	0	0	0	0	0	0	1	0
a_3	0	0	0	0	0	0	0	0	1

PerFunc	ß
0	1,575

Figure 9. Reliability analysis of the gravity foundation of an offshore wind energy converter using Microsoft Ecxcel spreadsheet

because of the fact that with F_1 = 125 kN the upper peak of the failure body is regarded here. If the vertical load would be much greater the load F_{10} would have a greater influence on the safety of the system. This may be visualized by changing the vertical load F_1. In the actual case of F_1 = 125 MN an index ß = 1.58 was determinated. For a load F_1 = 350 MN the index increases to ß = 2.93 and for a load F_1 = 600 MN the index decreases to ß = 1.34. In the last case the vertical failure load F_{10} and the soil friction angle have a greater influence on the system, because now the lower peak of the failure surface is considered here. Beyond it this example shows that the sytem gets safer by increasing the vertical load. But this is valid only up to a special point after that the safety of the system decreases.

5 DISPLACEMENTS AND ROTATIONS

In the following the calculation of the displacements and rotations of the gravity foundation under the load paths discussed before will be shown. For this example the soil conditons in the southern North Sea are taken into account. The submarine strata is characterized predominantly by non-cohesive soil layers of Pleistocene sediments which consist of medium dense to dense fine to medium sands (Wiemann et al. 2002).

At first the the initial and final stiffness of the corresponding load-displacement curve for a centric vertical load has to be determined. Here the formulation after Mayne & Poulos (2001) is used.

$$u_1 = q \cdot B \cdot I \cdot \frac{\left(1-\nu^2\right)}{E_{max} \cdot \left\{1-\left(\frac{q}{q_{ult}}\right)^{0,3}\right\}} \qquad (16)$$

Parameter	**value**
vertical load F_1 [MN]	103
horizontal load F_2 [MN]	16
torsional moment M_1 [MNm]	4
bending moment M_3 [MNm]	562
initial stiffness k_0 [MN/m]	2100
final stiffness k_f [MN/m]	5
plastic potential parameter c_1 [-]	4
plastic potential parameter c_2 [-]	5
plastic potential parameter c_3 [-]	5

Herein q is the applied stress and q_{ult} the ultimate stress from bearing capacity theory. The Poisson's ratio will be assumed to υ = 0.15 and the elastic modulus to E_{max} = 120 MN/m². The displacement influence factor I contains all geometrical and soil effects. All relevant data for the simulation are summrized in Table 1. Which also includes the parameters for the plastic potential after Equation 8. The required values can be taken from the determined curve and the displacements for the load path described in Figure 9 can be calculated. Here, the vertical load F_1 has been applied first and the three other loads have been increased simultaneously up to failure.

In Figure 10 the horizontal displacement u_2 of the foundation depending on the corresponding load component F_2 is shown. Figure 11 shows the rotation ω_3 and the horizontal displacement u_2 versus the settlement u_1. The vertical displacements starts at u_1 = 0.15 m. These settlement results from the vertical load F_1 and is calculated with Equation 16. The following settlements were released due to the additional load combinations.

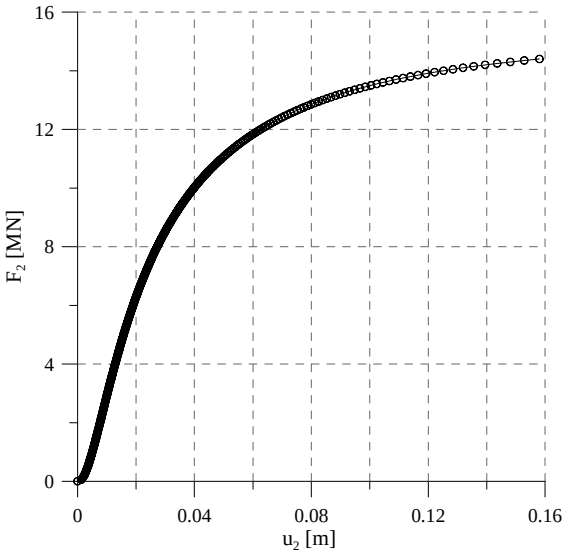

Figure 10. Load-displacement curve u_2-F_2 for a gravity foundation, calculated with the SSH-Model

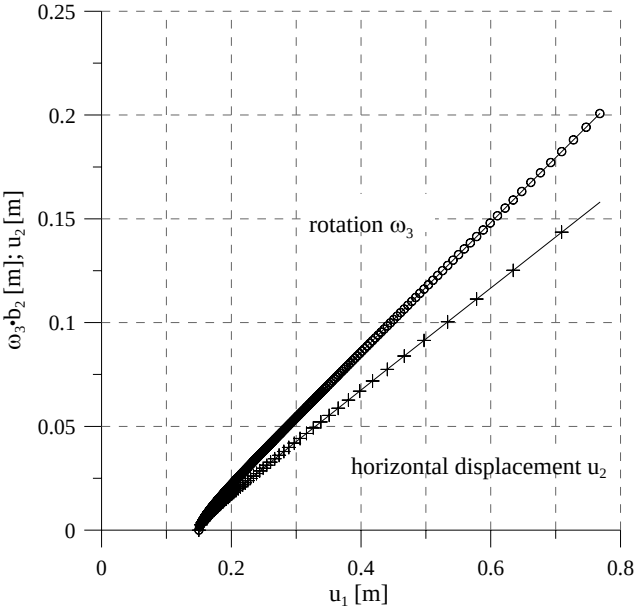

Figure 11. Settlement-displacement-curve u_1-u_2 and settlement-rotation-curve u_1-$\omega_3 \bullet b_2$ for a gravity foundation, calculated with the SSH-Model

6 CONCLUSION

A design method has been presented which describes the complex behaviour of shallow foundations under loading up to failure. The two components of this model, failure condition and corresponding displacement rule, consider both, ULS and SLS. Together with the methods proposed by Low (2005) and Phoon (2004) a practical application for the determination of the Hasofer-Lind index ß is formulated. With this formulation it is possible to indicate the safety of the system not only for the mean values but also in dependence of scatter and correlations of the parameters. The ability of the method was presented using a example of an offshore wind energy converter.

7 ACKNOWLEDGEMENT

The authors wish to thank the German National Research Council (DFG) for supporting this research work.

REFERENCES

Bay-Gress, C. 2000. *Etude de l´interaction sol – structure, comportement non lineare sol – fondation superficielle.* These Université Louis Pasteur, Strassburg (in french)

DIN EN 1997-1 2005. *Eurocode 7: Entwurf, Berechnung und Bemessung in der Geotechnik – Teil1: Allgemeine Regeln.* Berlin: Normenausschuss Bauwesen im Deutschen Institut fuer Normung e. V. (German version)

Hasofer, A. M. & Lind, N. C. 1974. An exact and invariant first order reliability format. *Journal of Enginnering Mechanics Division, ASCE* 100: 111-121

Lesny, K. 2001. *Entwicklung eines konsistenten Versagens-modells zum Nachweis der Standsicherheit flach-gegründeter Fundamente.* Mitteilungen aus dem Fachgebiet Grundbau und Bodenmechanik, Heft 27. Essen: Prof. Dr.-Ing. W. Richwien (in German)

Lesny, K.; Hinz, P. 2006: A concept for a Safe and Economic Design of Foundations for Offshore Wind Energy Converters. *New Approach to Harbour, Coastal Risk Management and Education, Proc. of LITTORAL 2006, Gdansk, Polen:* 90-98

Lesny, K., Kisse, A. & Richwien, W. 2002. Proof of Foundation Stabililty Using a Consistent Failure Model. *Proc. of the Int. Conf. on Probabilistics in Geotechnics - Technical and Economic Risk Estimation, Graz, Austria:* 95-103

Lesny, K & Richwien, W. 2002. A Consistent Failure Model for Single Footings embedded in Sand. *Proc. of the Int. Workshop on Foundation Design Codes and Soil Investigation in View of International Harmonization and Performance Based Design, Kamakura, Tokyo, Japan:* 159-165

Low, B. & Phoon, K.K. 2002. Practical first-order reliability computations using spreadsheet. *Proc. of the Int. Conf. on Probabilistics in Geotechnics: Technical and Economic Risk Estimation, Graz, Austria:* 93-46

Low, B. & Tang, W. H. 1997. Efficient reliability evaluation using spreadsheet. *Journal of Engineering Mechanics, ASCE* 123(7): 749-752

Low, B. & Tang, W. H. 2004. Reliability analysis using object oriented constrained optimization. *Structural Safety* 26: 69-89

Low, B. 2005. Reliability-based design applied to retaining walls. *Geotechnique* 55, No. 1: 63-75

Montrasio, L. 1994. *Un Metodo per il calcolo die cedimenti di fondazioni su sbbia soggette a carichi eccentrici e inclinati.* Dottorato di ricerca in Ingegneria Geotecnica, Università di Milano (in italian)

Phoon, K. K. 2004. *General Non-Gaussian Probability Models for First-Order Reliability Method (FORM): A Stte-of-the-Art Report. ICG Report 2004-2-4 (NGI Report 20031091-4)*, International Centre for Geohazards, Oslo

Wiemann, J., Lesny, K. & Richwien, W. 2002. *Gruendung von Offshore-Windenergieanlagen – Gruendungskonzepte und geotechnische Grundlagen.* Mitteilungen aus dem Fachgebiet Grundbau und Bodenmechanik, Heft 29. Essen: Prof. Dr.-Ing. W. Richwien (in German)

Zienkiewicz, O. C. 1988. *The Finite Element Method*. London: Mc Graw Hill